

A HIGHER ORDER SCHEME FOR THE CURVE SHORTENING FLOW OF PLANE CURVES

MARTIN BALAŽOVJECH * AND KAROL MIKULA †

Abstract. We introduce a new higher order scheme for computing the curve shortening flow represented by the intrinsic partial differential equation for updating the evolving curve position vector. Our new scheme is of the Crank-Nicolson-type, the key idea is in averaging of the first-order explicit forward Euler and fully-implicit backward Euler schemes. At any time step, the solution is found iteratively applying the semi-implicit approach. Interestingly, the new scheme gives exact solution for uniformly discretized shrinking circle which is not true for other known discrete schemes approximating the curve shortening flow. Study of experimental order of convergence shows its fourth order accuracy for nonuniformly discretized shrinking circle and we expect the second order accuracy in general, which is indicated by the second order experimental order of convergence (EOC) for evolution of the enclosed area. Together with the new scheme we present forward Euler and semi-implicit and fully-implicit backward Euler schemes and compare them regarding precision and computational efficiency. For all the schemes the spatial discretization is based on the flowing finite volume or mass lumped finite element methods.

Key words. geometric partial differential equations, evolving plane curves, mean curvature flow, curve shortening flow, finite element method, finite volume method, higher order scheme

AMS subject classifications. 35K65, 65N40, 53C80

1. Introduction. In this paper we introduce a new higher order scheme for computing the curve shortening flow equation

$$(1.1) \quad \partial_t \mathbf{r} = k\mathbf{n},$$

where $k\mathbf{n} = \partial_s \mathbf{t} = \partial_{ss} \mathbf{r}$ is the curvature vector and $\mathbf{r} = [x, y]$ is the position vector, which is a function of the arc-length parametrization s of a curve and time t . In the case of closed curves \mathbf{r} has to satisfy the periodic boundary conditions. The evolving curves are used in various applications ranging from physics to image processing [1, 10, 3, 11], their analysis was given in [7, 8] and numerical schemes of different type were presented e.g. in [5, 6, 4, 9, 12, 13, 14, 15, 16, 2].

If we use finite element approximation and mass lumping [5] or flowing finite volume approximation [14] we obtain following semidiscrete scheme

$$(1.2) \quad \frac{h_{i+1} + h_i}{2} \partial_t \mathbf{r}_i = \frac{\mathbf{r}_{i+1} - \mathbf{r}_i}{h_{i+1}} - \frac{\mathbf{r}_i - \mathbf{r}_{i-1}}{h_i}$$

where $\mathbf{r}_i = [x_i, y_i]^T$, $i = 1, \dots, n$, is a time dependent discrete solution and $h_i = |\mathbf{r}_i - \mathbf{r}_{i-1}|$ is Euclidean distance of spatial grid points. Due to periodic boundary conditions we will use also the additional values defined by $\mathbf{r}_0 = \mathbf{r}_n$, $\mathbf{r}_1 = \mathbf{r}_{n+1}$.

One can transform the scheme (1.2) into the set of linear algebraic equations in several different ways. We can obtain a first-order explicit forward Euler or first-order

*Department of Mathematics, Slovak University of Technology, Radlinského 11, 813 68 Bratislava, Slovak Republic (balazovjech@math.sk).

†Department of Mathematics, Slovak University of Technology, Radlinského 11, 813 68 Bratislava, Slovak Republic (mikula@math.sk).

semi-implicit backward Euler schemes, see e.g. [5, 14]. In this paper we introduce new higher order Crank-Nicolson-type scheme which is a combination of explicit forward and fully-implicit backward Euler schemes. It is efficient since only few semi-implicit iterations are necessary in fully-implicit backward Euler part. The semi-implicit linear systems can be solved efficiently using cyclic tridiagonal solver. We will describe all above mentioned algorithms and compare their accuracy on numerical examples.

2. Numerical schemes. In the scheme (1.2) we approximate the time derivative $\partial_t \mathbf{r}_i$ by the difference $\frac{\mathbf{r}_i^{m+1} - \mathbf{r}_i^m}{\Delta t}$ where the index $m = 1, \dots, \frac{T}{\Delta t} = M$, denotes discrete time stepping with a uniform time step Δt . In this way we can obtain the difference equations corresponding to equations (1.2). A type of the scheme depends on the choice of time approximation for all other terms in (1.2).

2.1. First-order explicit forward Euler scheme. It is given by the equations

$$(2.1) \quad \frac{h_{i+1}^m + h_i^m}{2} \frac{\mathbf{r}_i^{m+1} - \mathbf{r}_i^m}{\Delta t} = \frac{\mathbf{r}_{i+1}^m - \mathbf{r}_i^m}{h_{i+1}^m} - \frac{\mathbf{r}_i^m - \mathbf{r}_{i-1}^m}{h_i^m},$$

for $i = 1, \dots, n$ and periodic boundary conditions. Input values are represented by coordinates of position vector $\mathbf{r}_i^m = [x_i^m, y_i^m]$ in all nodes at the discrete time $t^m = m\Delta t$. First we compute distances of nodes

$$h_i^m = \sqrt{(x_i^m - x_{i-1}^m)^2 + (y_i^m - y_{i-1}^m)^2}.$$

Then we compute coordinates of the position vector $\mathbf{r}_i^{m+1} = [x_i^{m+1}, y_i^{m+1}]$ in the next time step $t^{m+1} = (m+1)\Delta t$ using

$$(2.2) \quad \mathbf{r}_i^{m+1} = \mathbf{r}_i^m + \frac{2\Delta t}{h_{i+1}^m + h_i^m} \left(\frac{\mathbf{r}_{i+1}^m - \mathbf{r}_i^m}{h_{i+1}^m} - \frac{\mathbf{r}_i^m - \mathbf{r}_{i-1}^m}{h_i^m} \right).$$

2.2. First-order semi-implicit backward Euler scheme. In this case we use the equations

$$(2.3) \quad \frac{h_{i+1}^m + h_i^m}{2} \frac{\mathbf{r}_i^{m+1} - \mathbf{r}_i^m}{\Delta t} = \frac{\mathbf{r}_{i+1}^{m+1} - \mathbf{r}_i^{m+1}}{h_{i+1}^m} - \frac{\mathbf{r}_i^{m+1} - \mathbf{r}_{i-1}^{m+1}}{h_i^m}.$$

Again the input values are represented by coordinates of position vector \mathbf{r}_i^m , $i = 1, \dots, n$ at time t^m , and we compute distances h_i^m of nodes. The new coordinates of the position vector \mathbf{r}_i^{m+1} are then determined by solving the cyclic tridiagonal system

$$(2.4) \quad -\frac{1}{h_i^m} \mathbf{r}_{i-1}^{m+1} + \left(\frac{h_{i+1}^m + h_i^m}{2\Delta t} + \frac{1}{h_{i+1}^m} + \frac{1}{h_i^m} \right) \mathbf{r}_i^{m+1} - \frac{1}{h_{i+1}^m} \mathbf{r}_{i+1}^{m+1} = \frac{h_{i+1}^m + h_i^m}{2\Delta t} \mathbf{r}_i^m.$$

2.3. First-order fully-implicit backward Euler scheme. It is given by the equations

$$(2.5) \quad \frac{h_{i+1}^{m+1} + h_i^{m+1}}{2} \frac{\mathbf{r}_i^{m+1} - \mathbf{r}_i^m}{\Delta t} = \frac{\mathbf{r}_{i+1}^{m+1} - \mathbf{r}_i^{m+1}}{h_{i+1}^{m+1}} - \frac{\mathbf{r}_i^{m+1} - \mathbf{r}_{i-1}^{m+1}}{h_i^{m+1}},$$

$i = 1, \dots, n$. In this scheme we use distances of nodes h_i^{m+1} at the time level t^{m+1} and not h_i^m . To obtain h_i^{m+1} we solve iteratively the following semi-implicit cyclic tridiagonal system

$$(2.6) \quad -\frac{1}{h_i^{m(l)}} \mathbf{r}_{i-1}^{m(l+1)} + \left(\frac{h_{i+1}^{m(l)} + h_i^{m(l)}}{2\Delta t} + \frac{1}{h_{i+1}^{m(l)}} + \frac{1}{h_i^{m(l)}} \right) \mathbf{r}_i^{m(l+1)} - \frac{1}{h_{i+1}^{m(l)}} \mathbf{r}_{i+1}^{m(l+1)} = \frac{h_{i+1}^{m(l)} + h_i^{m(l)}}{2\Delta t} \mathbf{r}_i^m,$$

where

$$h_i^{m(l)} = \sqrt{(x_i^{m(l)} - x_{i-1}^{m(l)})^2 + (y_i^{m(l)} - y_{i-1}^{m(l)})^2},$$

for $l = 0, 1, 2, \dots$. The iteration process is stopped, if a difference in length of two consecutive curves is less then prescribed tolerance, i.e. $|L^{m(l)} - L^{m(l+1)}| \leq \epsilon$. The length of the curve is computed as the sum of lengths of all elements, i.e. $L^{m(l)} = \sum_{i=1}^n h_i^{m(l)}$. For sufficiently small ϵ we use the last solution $\mathbf{r}_i^{m(l+1)}$, $i = 1, \dots, n$ as the approximation of \mathbf{r}_i^{m+1} , the solution of the scheme. Other stopping criteria would be also possible, but this one is computationally efficient because the lengths $h_i^{m(l)}$ are already computed when the criterion is evaluated.

2.4. The higher order scheme. It is a combination of (2.1) and (2.5), namely we use the equations

$$(2.7) \quad \frac{\mathbf{r}_{i+1}^m - \mathbf{r}_i^m}{h_{i+1}^m} - \frac{\mathbf{r}_i^m - \mathbf{r}_{i-1}^m}{h_i^m} + \frac{\mathbf{r}_{i+1}^{m+1} - \mathbf{r}_i^{m+1}}{h_{i+1}^{m+1}} - \frac{\mathbf{r}_i^{m+1} - \mathbf{r}_{i-1}^{m+1}}{h_i^{m+1}} = \frac{h_{i+1}^m + h_i^m + h_{i+1}^{m+1} + h_i^{m+1}}{2} \frac{\mathbf{r}_i^{m+1} - \mathbf{r}_i^m}{\Delta t},$$

$i = 1, \dots, n$. The input values are represented by coordinates of the position vector \mathbf{r}_i^m in all nodes. First we compute distances h_i^m and then we solve the system

$$(2.8) \quad -\frac{1}{h_i^{m(l)}} \mathbf{r}_{i-1}^{m(l+1)} + \left(\frac{h_{i+1}^{m(l)} + h_i^{m(l)} + h_{i+1}^m + h_i^m}{2\Delta t} + \frac{1}{h_{i+1}^{m(l)}} + \frac{1}{h_i^{m(l)}} \right) \mathbf{r}_i^{m(l+1)} - \frac{1}{h_{i+1}^{m(l)}} \mathbf{r}_{i+1}^{m(l+1)} = \left(\frac{h_{i+1}^{m(l)} + h_i^{m(l)} + h_{i+1}^m + h_i^m}{2\Delta t} - \frac{1}{h_{i+1}^m} - \frac{1}{h_i^m} \right) \mathbf{r}_i^m + \frac{\mathbf{r}_{i+1}^m}{h_{i+1}^m} + \frac{\mathbf{r}_{i-1}^m}{h_i^m}$$

in the same iterative way as for (2.6). The algorithm of the higher order scheme is depicted in Figure 2.1.

3. Numerical experiments. In this section we first test the schemes on the evolution of circle with initial uniform distribution of grid points given by

$$x_i = \cos(2\pi i/n), \quad y_i = \sin(2\pi i/n),$$

as well as with initial nonuniform distribution of grid points given by

$$x_i = \cos(2\pi i/n + 0.2 \sin(4\pi i/n)), \quad y_i = \sin(2\pi i/n + 0.2 \sin(4\pi i/n)),$$

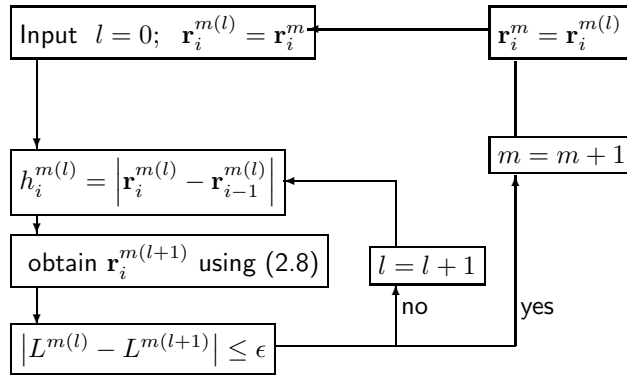


FIG. 2.1. Algorithm of computation of the higher order scheme

$i = 1, \dots, n$. We compare accuracy of the schemes with analytical solution where the time dependent radius $|\mathbf{r}(t)|$ of the shrinking circle is given by

$$(3.1) \quad |\mathbf{r}(t)| = \sqrt{\mathbf{r}(0)^2 - 2t}.$$

To estimate the error e_n^M we use numerical L_2 norm in the form

$$(3.2) \quad \|e_n^M\| = \sqrt{\sum_{m=1}^M \Delta t \sum_{i=1}^n (|\mathbf{r}_i^m| - |\mathbf{r}(m\Delta t)|)^2 \frac{h_i^m + h_{i+1}^m}{2}}.$$

The experimental order of convergence is then defined by

$$(3.3) \quad \text{EOC} = \log_2 \frac{\|e_n^M\|}{\|e_{2n}^{2M}\|}.$$

We computed the errors $\|e_n^M\|$ in the time interval $[0, T]$ with $T = 0.1$, $|\mathbf{r}(0)| = 1$, using $n = 10, 20, \dots$ grid points and decreasing correspondingly the time step Δt . The results for explicit forward Euler and semi-implicit backward Euler schemes are reported in Tables 3.1 and 3.2. We can see that both schemes are first order

TABLE 3.1

Numerical error and EOC for the shrinking circle using explicit forward Euler scheme with uniform and nonuniform initial distribution of grid points.

n	Δt	Uniform initial distribution		Nonuniform initial distribution	
		$\ e_n^M\ $	EOC	$\ e_n^M\ $	EOC
10	1.0000e-1	4.381071e-3		4.383950e-3	
20	5.0000e-2	1.764560e-3	1.31	1.764033e-3	1.31
40	2.5000e-2	7.671827e-4	1.20	7.670978e-4	1.20
80	1.2500e-2	3.537897e-4	1.12	3.537790e-4	1.12
160	6.2500e-3	4.016483e-2	-6.8	7.064467e-2	-7.64

accurate. For $n = 160$ and $\Delta t = 0.00625$ the stability of the explicit scheme is broken. In the Tables 3.3 and 3.4 we show errors and EOC for the fully-implicit backward Euler and our higher order scheme where we used as stopping criterion for iterations $\epsilon = 10^{-8}$. While the fully-implicit scheme is first order accurate, the higher order scheme shows in this example fourth order accuracy when the grid points

TABLE 3.2

Numerical error and EOC for the shrinking circle using semi-implicit backward Euler scheme with uniform and nonuniform initial distribution of grid points.

		Uniform initial distribution		Nonuniform initial distribution	
n	Δt	$\ e_n^M\ $	EOC	$\ e_n^M\ $	EOC
10	1.0000e-1	1.152790e-2		1.153664e-2	
20	5.0000e-2	4.929176e-3	1.23	4.928358e-3	1.23
40	2.5000e-2	2.217582e-3	1.15	2.217372e-3	1.15
80	1.2500e-2	1.041443e-3	1.09	1.041413e-3	1.09
160	6.2500e-3	5.031165e-4	1.05	5.031127e-4	1.05
320	3.1250e-3	2.470558e-4	1.03	2.470553e-4	1.03
640	1.5625e-3	1.223893e-4	1.01	1.223892e-4	1.01

are nonuniformly distributed. For the uniformly discretized circle the errors drop to machine precision limit (so we do not report EOC in this case) already for very coarse grids which is consequence of the statement in the following theorem.

TABLE 3.3

Numerical error and EOC for the shrinking circle using fully-implicit backward Euler scheme with uniform and nonuniform initial distribution of grid points.

		Uniform initial distribution		Nonuniform initial distribution	
n	Δt	$\ e_n^M\ $	EOC	$\ e_n^M\ $	EOC
10	1.0000e-1	5.279112e-3		5.283129e-3	
20	5.0000e-2	1.928786e-3	1.45	1.928205e-3	1.45
40	2.5000e-2	8.011272e-4	1.27	8.010384e-4	1.27
80	1.2500e-2	3.614162e-4	1.15	3.614053e-4	1.15
160	6.2500e-3	1.711187e-4	1.08	1.711174e-4	1.08
320	3.1250e-3	8.318585e-5	1.04	8.318569e-5	1.04
640	1.5625e-3	4.100247e-5	1.02	4.100245e-5	1.02

TABLE 3.4

Numerical error and EOC for the shrinking circle using our higher order scheme with uniform and nonuniform initial distribution of grid points.

		Uniform initial distribution		Nonuniform initial distribution	
n	Δt	$\ e_n^M\ $	EOC	$\ e_n^M\ $	EOC
10	1.0000e-1	1.563145e-11		1.550446e-05	
20	5.0000e-2	2.175665e-12		1.060490e-06	3.87
40	2.5000e-2	6.527264e-13		6.192806e-08	4.10
80	1.2500e-2	3.411833e-13		3.630243e-09	4.09
160	6.2500e-3	5.330244e-14		2.178424e-10	4.06
320	3.1250e-3	2.268496e-14		1.332024e-11	4.03
640	1.5625e-3	1.020198e-15		8.228928e-13	4.02

THEOREM 3.1. *The higher order scheme (2.7) gives the exact solution for any uniformly discretized initial circle using any length of the time step $\Delta t \leq (r^0)^2/2$, where r^0 is the initial radius.*

Proof. Let the initial circle be given by $\mathbf{r}_i^0 = (x_i^0, y_i^0) = r^0(\cos \varphi_i, \sin \varphi_i)$, $\varphi_i = i\varphi$, $\varphi = 2\pi/n$, $i = 1, \dots, n$. Let us have any cyclic tridiagonal matrix with diagonal coefficient equals to a and upper and lower diagonal coefficients equal to b , where a and b are given constants. By simple calculations

$$b \cos \varphi_{i-1} + a \cos \varphi_i + b \cos \varphi_{i+1} = b \cos(\varphi_i - \varphi) + a \cos \varphi_i + b \cos(\varphi_i + \varphi) =$$

$$b(\cos \varphi_i \cos \varphi + \sin \varphi_i \sin \varphi) + a \cos \varphi_i + b(\cos \varphi_i \cos \varphi - \sin \varphi_i \sin \varphi) = (a + 2b \cos \varphi) \cos \varphi_i,$$

and similarly for terms with sine replacing cosine function above, we get that x and y coordinates of uniformly discretized circle form the eigenspace of such matrices with the common eigenvalue $(a + 2b \cos \varphi)$.

Let us take any time step m and assume uniform distribution of grid points, i.e. $h_i^m = h^m$. Then let us also assume that $h_i^{m(l)} = h^{m(l)}$, $i = 1, \dots, n$, i.e. uniform discretization is given in any l -th iteration. In fact, the assumptions hold for $m = 0, l = 0$. Then the equation (2.8) has the following form

$$(3.4) \quad -\frac{1}{h^{m(l)}} \mathbf{r}_{i-1}^{m(l+1)} + \left(\frac{h^{m(l)} + h^m}{\Delta t} + \frac{2}{h^{m(l)}} \right) \mathbf{r}_i^{m(l+1)} - \frac{1}{h^{m(l)}} \mathbf{r}_{i+1}^{m(l+1)} = \frac{\mathbf{r}_{i-1}^m}{h^m} + \left(\frac{h^{m(l)} + h^m}{\Delta t} - \frac{2}{h^m} \right) \mathbf{r}_i^m + \frac{\mathbf{r}_{i+1}^m}{h^m}.$$

If we set $a = \frac{h^{m(l)} + h^m}{\Delta t} + \frac{2}{h^{m(l)}}$, $b = -\frac{1}{h^{m(l)}}$, $d = \frac{h^{m(l)} + h^m}{\Delta t} - \frac{2}{h^m}$, $e = \frac{1}{h^m}$, we obtain from (3.4) the cyclic tridiagonal system with constant coefficients (on the left as well as on the right hand side)

$$(3.5) \quad b \mathbf{r}_{i-1}^{m(l+1)} + a \mathbf{r}_i^{m(l+1)} + b \mathbf{r}_{i+1}^{m(l+1)} = e \mathbf{r}_{i-1}^m + d \mathbf{r}_i^m + e \mathbf{r}_{i+1}^m.$$

From the eigenspace properties it is clear that in the new iteration the vector $\mathbf{r}^{m(l+1)}$ represents again a uniformly discretized circle and thus $h_i^{m(l+1)} = h^{m(l+1)}$. By induction argument we get that at any time step and any iteration we get as a solution of the scheme uniformly discretized circle.

Moreover, if $\mathbf{r}_i^m = r^m (\cos \varphi_i, \sin \varphi_i)$ and $\mathbf{r}_i^{m(l+1)} = r^{m(l+1)} (\cos \varphi_i, \sin \varphi_i)$, $i = 1, \dots, n$, then $h^m = 2r^m \sin(\varphi/2)$, $r^{m(l+1)} = \lambda^{m(l)} r^m$ and $h^{m(l+1)} = 2r^{m(l+1)} \sin(\varphi/2) = \lambda^{m(l)} h^m$, where the scaling factor $\lambda^{m(l)}$ is given by the ratio of eigenvalues

$$\begin{aligned} \lambda^{m(l)} &= \frac{d + 2e \cos \varphi}{a + 2b \cos \varphi} = \frac{\frac{h^{m(l)} + h^m}{\Delta t} - \frac{2}{h^m} (1 - \cos \varphi)}{\frac{h^{m(l)} + h^m}{\Delta t} + \frac{2}{h^{m(l)}} (1 - \cos \varphi)} = \\ &= \frac{\lambda^{m(l-1)} (\lambda^{m(l-1)} + 1) (h^m)^2 - 2\Delta t \lambda^{m(l-1)} (1 - \cos \varphi)}{\lambda^{m(l-1)} (\lambda^{m(l-1)} + 1) (h^m)^2 + 2\Delta t (1 - \cos \varphi)} = \\ &= \frac{\lambda^{m(l-1)} (\lambda^{m(l-1)} + 1) (r^m)^2 - \lambda^{m(l-1)} \Delta t}{\lambda^{m(l-1)} (\lambda^{m(l-1)} + 1) (r^m)^2 + \Delta t} \end{aligned}$$

where the relation $2 \sin^2(\varphi/2) = (1 - \cos \varphi)$ was used in the last equality. We define $\lambda^{m(-1)} = 1$ as a starting point of such iterative process representing our scheme for uniformly discretized circle at the m th time step. Now we can define the function

$$g(\lambda) = \frac{\lambda(\lambda + 1)(r^m)^2 - \lambda \Delta t}{\lambda(\lambda + 1)(r^m)^2 + \Delta t}$$

for which $0 \leq g(\lambda) < 1$ hold for $\lambda \in [0, 1]$. Among the positive numbers this mapping has a fixed point $g(\lambda^*) = \lambda^*$ which is equal to

$$(3.6) \quad \lambda^* = \sqrt{1 - \frac{2\Delta t}{(r^m)^2}}$$

and is well defined if

$$(3.7) \quad \Delta t \leq \frac{(r^m)^2}{2}.$$

Let us denote $c_1 = (r^m)^2$, $c_2 = \Delta t$. Then the derivatives of g have the form

$$g'(\lambda) = \frac{c_1 c_2 (1+x)^2 - c_2^2}{(c_1 \lambda (\lambda + 1) + c_2)^2}$$

$$g''(\lambda) = \frac{1}{(c_1 \lambda (\lambda + 1) + c_2)^3} (-2c_1^2 c_2 - 6c_1^2 c_2 x - 6c_1^2 c_2 x^2 - 2c_1^2 c_2 x^3 + 4c_1 c_2^2 + 6c_1 c_2^2 x).$$

Provided $c_2 \leq \frac{c_1}{2}$, which is nothing else than condition (3.7), the function g is increasing and concave on interval $[0, 1]$ and $g(0) = 0$, $g(1) < 1$. From there it is clear that derivative of g must be strictly less than 1 in interval $[\lambda^*, 1]$ which means that g is a contraction on that interval. Since we start the fixed point iterations by $\lambda = 1$ we get by the Banach fixed point theorem that our iterative process converges to the fixed point λ^* . This means that the solution at the new time step is uniformly distributed circle with radius given by

$$(3.8) \quad r^{m+1} = \lambda^* r^m = \sqrt{(r^m)^2 - 2\Delta t}.$$

Comparing (3.8) with (3.1) we proved the theorem. \square

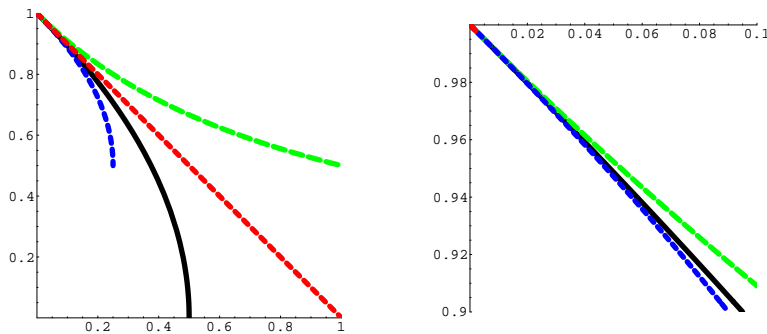


FIG. 3.1. A dependence of the computed radius (vertical axes) on Δt (horizontal axes) using one time step in the numerical schemes starting by the unit circle. Bold black line - the solution by the higher order scheme coincides with the exact solution for any Δt . Green (in electronic version) line with larger dashing - semi-implicit scheme, which is the most slow. Blue (in electronic version) line with shorter dashing - fully-implicit scheme, which is the most fast. Red (in electronic version) line with shorter dashing - explicit scheme, which is slower than exact solution and has strong stability constraint. In the right part we see it as a short (red) line only on the interval of stability. The dependence curves of the other schemes are also plotted there, to see their behaviour for reasonably short time steps.

Remark. The statement in Theorem 3.1 does not hold for any of the explicit, semi-implicit or fully-implicit schemes. In fact, the reader can verify using the same strategy as above, that we have $r^{m+1} = r^m - \frac{\Delta t}{r^m}$ for the explicit scheme, $r^{m+1} = \frac{(r^m)^3}{(r^m)^2 + \Delta t}$ for the semi-implicit scheme and $r^{m+1} = \frac{r^m + \sqrt{(r^m)^2 - 4\Delta t}}{2}$ for the fully-implicit scheme.

Just for an illustration, how the error depends on Δt in one time step of the schemes, we plot those curves for the case of initial unit circle in Fig. 3.1 left. The exact solution and the numerical solution by the higher order scheme coincide for any length of the time step and it is plotted by the bold line. The other schemes cannot be exact for any choice of the time step. They have the same slope initially, so they give comparable accuracy (same EOC) for reasonably small time steps as documented in Tables 3.1-3.3. For large time steps they would differ significantly in correct speed of shrinking. Moreover in this case, the explicit scheme has strong stability constraint, $\Delta t \leq (h^m)^2/2$, which is documented in Fig. 3.1 right for $n = 100$. It may become very restrictive in general curve shortening, when Δt must be less or equal to $\min_i (h_i^m)^2/2$ to guarantee the stability of explicit scheme. The other two schemes can be used without losing stability for large time steps but one has to take into account the error increase as plotted in Fig. 3.1 right. The optimal choice regarding accuracy and stability is the higher order scheme (2.7) which is discussed also in the next two experiments.

In the next experiment we test our higher order scheme in the evolution of ellipse represented by 200 grid points with initial distribution given by

$$x_i = 2 \cos(2\pi i/n + 0.125 \sin(4\pi i/n)), \quad y_i = \sin(2\pi i/n + 0.125 \sin(4\pi i/n)),$$

$i = 1, \dots, n$. We compare accuracy of the presented scheme with the reference solution \mathbf{r}^{ref} computed using explicit forward Euler scheme with very small time step $\Delta t = 10^{-7}$. The error was measured by difference in the maximum norm in the final time $T = 0.1$ by

$$(3.9) \quad \|e\| = \max_i \left| \mathbf{r}_i(T) - \mathbf{r}_i^{ref}(T) \right|.$$

Moreover, we measured CPU-times for computations with different parameters in order to reach a prescribed difference with the reference solution. Table 3.5 shows the error (distance from the reference solution) and CPU times for the explicit scheme and Table 3.6 for the higher order scheme. We can see that the higher order scheme gives the corresponding error using much larger time step and consequently in much shorter CPU time. E.g., we can see that the error of order $7.5 \cdot 10^{-7}$ was obtained by the higher order scheme in computation which took 0.078 sec. while for the explicit scheme it was in more than 10 sec.

TABLE 3.5

Difference from the reference solution in maximum norm and CPU-times for the shrinking ellipse using the explicit forward Euler scheme.

Δt	$\ e\ $	CPU - time (s)
1.00000e-5	1.932696e - 6	0.25
1.00000e-6	9.663479e - 7	2.625
2.50000e-7	7.580254e - 7	10.453
1.00000e-7	0	26.14

In a similar experiment we present time evolution of the nonconvex curve for which

$$x_i = \cos(z), \quad y_i = 0.5 \sin(z) + \sin(x_i) + \sin(z) (0.2 + \sin(z) \sin^2(3z)),$$

$z = 2\pi i/n, i = 1, \dots, n, n = 300$. We computed again the reference solution, now due to stability reasons, using the semi-implicit backward Euler scheme with small

TABLE 3.6

Difference from the reference solution in maximum norm and CPU-times for the shrinking ellipse using the higher order scheme.

Δt	$\ e\ $	CPU - time (s)
1.25000e-2	2.116709e -5	0.012
6.25000e-3	5.525566e -6	0.015
3.12500e-3	2.155265e -6	0.020
1.56250e-3	1.174023e -6	0.031
7.81250e-4	9.653597e - 7	0.047
3.90625e-4	6.034250e - 7	0.078

time step $\Delta t = 0.000025$. Then we compare precision of the higher order scheme and semi-implicit scheme using for both schemes bigger time step $\Delta t = 0.0025$. In Figure 3.2 we present computational results for both schemes in time moments $m\Delta t, m = 0, 30, 60, 90, 120$. In Figure 3.3 we compare both solutions in the terminal time $T = 120\Delta t = 0.3125$ where in the zoom (right picture) one can clearly see high precision of the scheme (2.7).

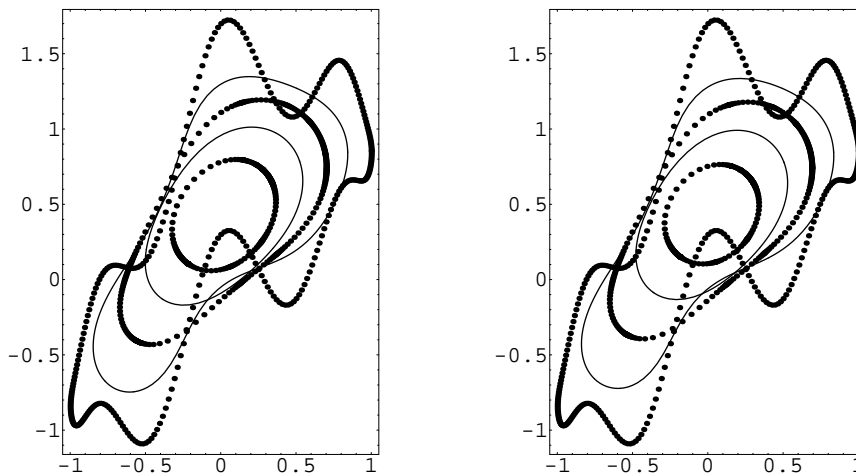


FIG. 3.2. The time evolution of the nonconvex curve computed by semi-implicit scheme (left) and our higher order scheme (right); the semi-implicit scheme is slower using the same time step.

In the last experiment we test our higher order scheme comparing the numerical and analytical evolutions of enclosed area in the curve shortening flow. We report results for the same evolving ellipse and nonconvex curve as used above in the time interval $[0, T]$, with $T = 0.1$, using $n = 50, 100, \dots$ grid points and decreasing correspondingly the time step Δt . As the error measure we use

$$(3.10) \quad \|\epsilon_n^M\| = \sqrt{\sum_{m=1}^M (A_n^m - A(m\Delta t))^2 \Delta t},$$

where $A_n^m = \frac{1}{2} \sum_{i=1}^n x_i^m (y_i^m - y_{i-1}^m) - y_i^m (x_i^m - x_{i-1}^m)$ is the area of discrete curve at the m -th time step and the exact area evolution is given by $A(t) = A(0) - 2\pi t$ where

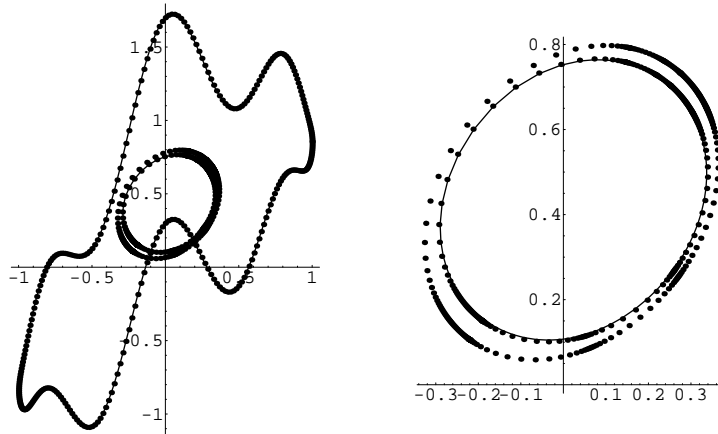


FIG. 3.3. Comparison of solutions by the higher order and semi-implicit schemes with the reference solution at the terminal time $T = 0.3125$. By the solid line we plot the reference solution, very close to this one is the solution by the higher order scheme and the semi-implicit scheme gives the result with much bigger error.

we use $A(0) = A_n^0$, the area of initial polygonal curve. The area evolution errors and EOC are reported in Table 3.7, we can see that our scheme is second order accurate with respect to this important quantity. Naturally, all other schemes discussed in this paper are at most first order accurate.

TABLE 3.7

The numerical errors in enclosed area and EOC for the evolving ellipse and nonconvex curve using our higher order scheme.

n	Δt	Ellipse		Nonconvex curve	
		$\ e_n^M\ $	EOC	$\ e_n^M\ $	EOC
50	3.125000e-003	6.815650e-004		5.819859e-003	
100	1.562500e-003	1.693104e-004	2.00918	1.755853e-003	1.72881
200	7.812500e-004	4.215025e-005	2.00606	4.887627e-004	1.84497
400	3.906250e-004	1.051220e-005	2.00348	1.269045e-004	1.94539
800	1.953125e-004	2.624707e-006	2.00184	3.206530e-005	1.98466
1600	9.765625e-005	6.557476e-007	2.00094	8.044106e-006	1.99501
3200	4.882813e-005	1.638824e-007	2.00048	2.016388e-006	1.99616

REFERENCES

- [1] S. B. ANGENENT, M. E. GURTIN, *Multiphase thermomechanics with an interfacial structure 2. Evolution of an isothermal interface*, Arch. Rat. Mech. Anal., 108 (1989), pp. 323–391.
- [2] J. W. BARRETT, H. GARCKE, R. NÜRNBERG, *On the variational approximation of combined second and fourth order geometric evolution equations*, SIAM J. Sci. Comput., 29 (2007) pp. 1006–1041.
- [3] V. CASELLES, R. KIMMEL, G. SAPIRO, *Geodesic active contours*, International Journal of Computer Vision, 22 (1997), pp. 61–79.
- [4] K. DECKELNICK, *Weak solutions of the curve shortening flow*, Calc. Var. Partial Differential Equations, 5 (1997), pp. 489–510.
- [5] G. DZIUK, *Convergence of a semi discrete scheme for the curve shortening flow*, Mathematical Models and Methods in Applied Sciences, 4 (1994), pp. 589–606.

- [6] G. DZIUK, *Discrete anisotropic curve shortening flow*, SIAM J. Numer. Anal., 36 (1999), pp. 1808–1830.
- [7] M. GAGE, R. S. HAMILTON, *The heat equation shrinking convex plane curves*, J. Diff. Geom., 23 (1986), pp. 69–96.
- [8] M. GRAYSON, *The heat equation shrinks embedded plane curves to round points*, J. Diff. Geom., 26 (1987), pp. 285–314.
- [9] T.Y. HOU, J. LOWENGRUB, M. SHELLEY, *Removing the stiffness from interfacial flows and surface tension*, J. Comput. Phys., 114 (1994), pp. 312–338.
- [10] M. KASS, A. WITKIN, D. TERZOPULOS, *Snakes: active contour models*, International Journal of Computer Vision, 1 (1987), pp. 321–331.
- [11] S. KICHENASSAMY, A. KUMAR, P. OLVER, A. TANNENBAUM, A. YEZZI, *Conformal curvature flows: from phase transitions to active vision*, Arch. Rational Mech. Anal., 134 (1996), pp. 275–301.
- [12] M. KIMURA, *Numerical analysis for moving boundary problems using the boundary tracking method*, Japan J. Indust. Appl. Math., 14 (1997), pp. 373–398.
- [13] K. MIKULA, J. KAČUR, *Evolution of convex plane curves describing anisotropic motions of phase interfaces*, SIAM J. Sci. Comput., 17 (1996), pp. 1302–1327.
- [14] K. MIKULA, D. ŠEVČOVIČ, *Evolution of plane curves driven by a nonlinear function of curvature and anisotropy*, SIAM J. Appl. Math., 61 (2001), pp. 1473–1501.
- [15] K. MIKULA, D. ŠEVČOVIČ, *A direct method for solving an anisotropic mean curvature flow of planar curve with an external force*, Mathematical Methods in Applied Sciences, 27 (2004) pp. 1545–1565.
- [16] K. MIKULA, D. ŠEVČOVIČ, *Tangentially stabilized Lagrangean algorithm for elastic curve evolution driven by intrinsic Laplacian of curvature*, ALGORITMY 2005, Conference on Scientific Computing, Vysoke Tatry-Podbanske, Slovakia, March 13-18, 2005, Proceedings of contributed papers and posters (2005), pp. 32–41.